

Study of Higgs plus single top production using events with a same sign dimuon at the Large Hadron Collider

Departamento de Investigación en Física
Maestría en Ciencias (Física)
Hiram Ernesto Damián

Universidad de Sonora

October 28, 2019



Contenido

- 1 Overview and motivation
 - 2 Higgs theory
 - 3 tH mechanisms
 - 4 Production cross section
 - 5 Higgs Branching ratios
 - 6 Fitting
 - 7 Results
 - 8 Conclusions
 - 9 References
 - 10 Supportive slides



Overview

- Through this project we will investigate the production of Higgs boson in association with a single top quark (tH) in proton-proton collisions. This mechanism of production of the Higgs boson has not been observed before by any experiment.
 - Understanding the production of the Higgs boson, as well as its decays are an important part of the physical program of the CERN international laboratory experiments that try to complete the tests to verify the Standard Model, the theory of the fundamental particles
 - Making predictions for future measurements.



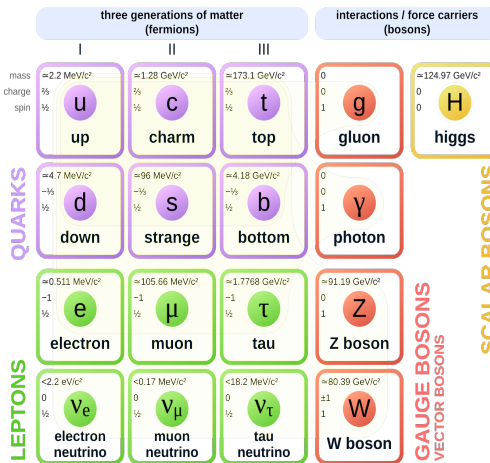
Motivation for single top Higgs (tH)

- Coupling measurement is essential to establish the nature of the Higgs
 - The exploration of Higgs production on the tH channel is subject relatively new. Measurements of CMS and ATLAS are compatible with SM predictions.
 - The tH study explores the relative sign of top-Higgs and W-Higgs couplings.
Small deviations from SM predictions could be associated with physics beyond the standard model (BSM) such as String Theory and Supersymmetry.



Standard Model

Standard Model of Elementary Particles



Particles Properties

Table of particles in SM

Particle	Mass (MeV/c ²)	Charge	spin	Lifetime (s)	Distance in lifetime (meters)
Up (<i>u</i>)	2.2	$\frac{2}{3}$	$\frac{1}{2}$	stable	-
Charm (<i>c</i>)	1280	$\frac{2}{3}$	$\frac{1}{2}$	1.1×10^{-12}	5.21×10^{-3}
Top (<i>t</i>)	173100	$\frac{2}{3}$	$\frac{1}{2}$	5×10^{-25}	2.37×10^{-15}
Down (<i>d</i>)	4.6	$-\frac{1}{3}$	$\frac{1}{2}$	Stable	-
Strange (<i>s</i>)	96	$-\frac{1}{3}$	$\frac{1}{2}$	1.24×10^{-8}	58.7
Bottom (<i>b</i>)	4180	$-\frac{1}{3}$	$\frac{1}{2}$	1.3×10^{-12}	6.16×10^{-3}
<i>W</i>	80379	± 1	1	3×10^{-25}	1.42×10^{-15}
<i>Z</i>	91187.6	0	1	3×10^{-25}	1.42×10^{-15}
Photon (γ)	0	0	1	Stable	-
Gluon (<i>g</i>)	0	0	1	Stable	-
Higgs (<i>H</i>)	125.18	0	0	1.56×10^{-22}	7.39×10^{-13}
Electron (<i>e</i>)	0.511	-1	$\frac{1}{2}$	Stable	-
Muon (<i>μ</i>)	105.7	-1	$\frac{1}{2}$	2.2×10^{-6}	10419.85
τ	1776.86	-1	$\frac{1}{2}$	2.9×10^{-13}	1.37×10^{-3}
ν_e ν_μ ν_τ	0	0	$\frac{1}{2}$	Stable	-



Electroweak SM Lagrangian

The Standard Model is a theory of fields for particles with spins 0, $\frac{1}{2}$ and 1. The SM lagrangian

$$\mathcal{L} = \mathcal{L}_{\text{gauge}} + \mathcal{L}_f + \mathcal{L}_{\text{higgs}} + \mathcal{L}_{\text{yukawa}}$$

donde

- $\mathcal{L}_{\text{gauge}} = -\frac{1}{4} [F^{\mu\nu} F_{\mu\nu}] - \frac{1}{4} [G^{i\mu\nu} G^i_{\mu\nu}]$
 - $F^{\mu\nu} = \partial_\mu B_\nu - \partial_\nu B_\mu$
 - $G^{i\mu\nu} = \partial_\mu W_\nu^i - \partial_\nu W_\mu^i - g \epsilon^{ijk} W_\mu^j W_\nu^k$
 - $\mathcal{L}_f = i\bar{\Psi}_L \not{D} \Psi_L + i\bar{\psi}_R \not{D} \psi_R$ is the kinematic term for fermions
 - $D_\mu \Psi_L = (\partial_\mu + igW_\mu + ig'Y_L B_\mu) \Psi_L$
 - $D_\mu \psi_R = (\partial_\mu + ig'Y_R B_\mu) \psi_R$
 - g and g' are boson coupling constants.
 - $W_\mu = \sigma^i W_\mu^i$, where σ^i are the pauli matrices.



Electroweak SM Lagrangian

Higgs lagrangian

$$\mathcal{L}_{\text{Higgs}} = (D_\mu \Phi)^\dagger (D^\mu \Phi) - V(\Phi^\dagger \Phi) \quad (1)$$

with

- $D_\mu \Phi = \left(\partial_\mu + (ig/2)\sigma^i W_\mu^i - i\frac{1}{2}g' B_\mu \right) \Phi$
 - $V(\Phi^\dagger \Phi) = -\mu^2 \Phi^\dagger \Phi + \frac{1}{2}\lambda (\Phi^\dagger \Phi)^2, \quad \mu^2 > 0$
 - $\Phi = \begin{pmatrix} \phi^+ \\ \phi^0 \end{pmatrix}$ is a SU(2) doublet.
 - σ^i are the Pauli matrices.
 - Φ is higgs field which is a complex scalar field. Φ
 - λ and μ^2 are Higgs potential parameters



SM Lagrangian

Yukawa lagrangian

$$\mathcal{L}_{yukawa} = \Gamma_{mn}^u q_{m,L} \tilde{\phi} u_{n,R} + \Gamma_{mn}^d \bar{q}_{m,L} \phi d_{n,R} + \Gamma_{mn}^e \bar{l}_{m,L} \phi e_{n,R} + h.c \quad (2)$$

where $h.c$ is hermitian conjugate. m and n are flavors of quarks and leptons.

The matrices Γ_{mn} describe the so called Yukawa couplings between higgs doublet ϕ and the fermions.

Choosing

$$\Phi = -\frac{1}{2} \begin{pmatrix} 0 \\ v+h \end{pmatrix} \rightarrow \Phi = \frac{1}{2} \begin{pmatrix} 0 \\ v \end{pmatrix}$$

By using it on the first part of the lagrangian it is obtained for u quark

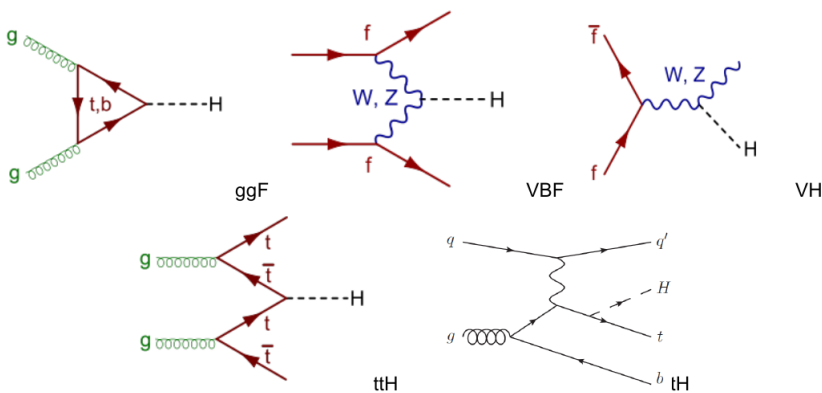
$$\mathcal{L}_{yukawa} = \frac{\Gamma_{uu}^u v}{\sqrt{2}} (\bar{u}_L u_R + \bar{u}_R u_L)$$

from here the mass of u quark

$$m_u = -\frac{\Gamma_{uu}^u v}{\sqrt{2}}$$



Higgs production mechanisms



Different Higgs production mechanism, from the most likely to least likely

tH production mechanisms

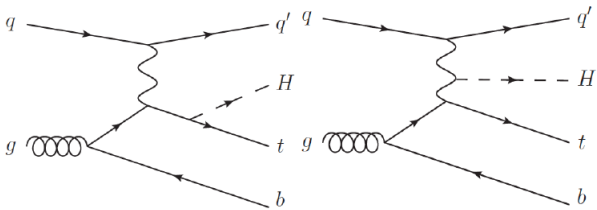


Figure: tH mechanism. Higgs radiated from a top quark (left). Higgs radiated from a W boson (right)

tH production mechanisms

- In a proton proton collision, the production cross section of the single top plus Higgs boson process is driven by a destructive interference of two main diagrams (see Fig. 1.), where the Higgs couples to either the W boson or the top quark.
 - A second process, where the Higgs and top quark are accompanied by a W boson (tHW) has similar behavior, albeit with a weaker interference pattern.
 - However, in the presence of new physics, there may be relative opposite signs between the tH and WH couplings which lead to constructive interference and enhance the cross sections by an order of magnitude or more.

Cross section

- Cross section describes the likelihood of two particles interacting under certain conditions[1][8]
 - Experimentally

$$d\sigma = \frac{\text{number of particles scattered into solid angle } \Delta\Omega}{(\text{number of particles incident})(\text{scattering centers/area})} \quad (3)$$

- Cross sections are expressed in barns , where $1 \text{ barn} = 10^{-28} \text{ cm}^{-2}$
 - The reaction rate N_R is determined by the total cross section σ and the incident flux L.
L is called luminosity and it is measured in $\text{cm}^{-1}\text{s}^{-1}$.[8]

$$N_R = \sigma L \quad (4)$$

Higgs production Cross section

Higgs boson production cross sections in pp collisions for $\sqrt{s} = 13\text{TeV}$ (in pico barn). Integrated luminosity of 35.9 fb^{-1} for Run 2¹

Production mechanism	σ (picobarns pb)	Number of events
ggF	48.93	1756587
VBF	3.78	135702
WH	1.35	48465
ZH	0.88	31592
t <bar>t>H</bar>	0.50	18255
tH (only)	0.015	560.39

¹Data taken from The cern collaborarion "Higgs Physics the HL-LHC and HE-LHC" 2019, CERN-LPCC-2018-04

Branching ratio

In particle physics, the branching ratio for a decay process is the ratio of the number of particles which decay via a specific decay mode with respect to the total number of particles which decay via all decay modes.

$$\text{BR} = \frac{\Gamma_i}{\sum_i \Gamma_i} \quad (5)$$

Where $\Gamma = \sum_i \Gamma_i$ is the total decay width (sum of all partial widths) of the particle and is related to lifetime of the particle: $\Gamma = 1/\tau$. Since the dimension of Γ is the inverse of time, in our system of natural units, it is measured in inverse seconds.⁰

⁰Cleaves H.J. (2011) Branching Ratio. In: Gargaud M. et al. (eds) Encyclopedia of Astrobiology. Springer, Berlin, Heidelberg

Higgs Branching ratios per channel

SM Higgs boson branching ratios for $M_H = 125$ GeV

Higgs decay	Branching ratio (BR)
$H \rightarrow b\bar{b}$	50.82%
$H \rightarrow W^+W^-$	21.5%
$H \rightarrow \tau^+\tau^-$	6.27%
$H \rightarrow ZZ$	2.61%
$H \rightarrow \gamma\gamma$	0.227%
$H \rightarrow Z\gamma$	0.153%
$H \rightarrow \mu^+\mu^-$	0.0217%

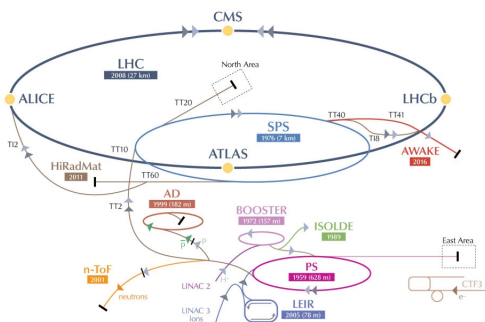
$\mu\mu$ same sign decay rate

Table of decay chains for tH. Expected number of final events assuming 560 produced tH events. I represents μ^\pm, e^\pm, τ^\pm .

Decay chain	BR	Events
$tH \rightarrow W^+ b W^+ W^- \rightarrow \mu^+ \nu_\mu b \mu^+ \nu_\mu q \bar{q}'$	2.096×10^{-3}	1.173
$tH \rightarrow W^+ b W^+ W^- \rightarrow \mu^+ \nu_\mu b \mu^+ \nu_\mu l^- \bar{\nu}_l$	3.37×10^{-4}	0.899
$tH \rightarrow W^+ b \tau^+ \tau^- \rightarrow \mu^+ \nu_\mu b \mu^+ \nu_\mu \bar{\nu}_\tau l^- \bar{\nu}_l \nu_\tau$	3.637×10^{-4}	0.203
$tH \rightarrow W^+ b W^+ W^- \rightarrow \tau^+ \bar{\nu}_\tau b \mu^+ \nu_\mu q \bar{q} \rightarrow \mu^+ \nu_\mu \bar{\nu}_\tau \bar{\nu}_\tau b \mu^+ \nu_\mu q \bar{q}$	1.890×10^{-4}	0.105
$tH \rightarrow W^+ b \tau^+ \tau^- \rightarrow \mu^+ \nu_\mu b \nu_\tau \mu^+ \nu_\mu \bar{\nu}_\tau q \bar{q}$	1.681×10^{-4}	0.094
$tH \rightarrow W^+ b W^+ W^- \rightarrow \tau^+ \bar{\nu}_\tau b \mu^+ \nu_\mu l^- \bar{\nu}_l \rightarrow \mu^+ \nu_\mu \bar{\nu}_\tau \bar{\nu}_\tau b \mu^+ \nu_\mu l^- \bar{\nu}_l$	3.045×10^{-5}	0.017
$tH \rightarrow W^+ b ZZ \rightarrow q \bar{q} b ZZ \rightarrow q \bar{q} b \mu^+ \mu^- \mu^+ \mu^-$	1.966×10^{-5}	0.011
$tH \rightarrow W^+ b \tau^+ \tau^- \rightarrow \tau^+ \bar{\nu}_\tau b \mu^+ \nu_\mu \bar{\nu}_\tau q \bar{q}' \nu_\tau \rightarrow \mu^+ \nu_\mu \bar{\nu}_\tau \bar{\nu}_\tau b \mu^+ \nu_\mu \bar{\nu}_\tau q \bar{q}' \nu_\tau$	1.549×10^{-5}	0.008

LHC

CERN's Accelerator Complex



LHC parameters

Quantity	Number
Circumference	26 659 m
Dipole operating temperature	1.9 K (-271.3°C)
Number of magnets	9593
Number of main dipoles	1232
Number of main quadrupoles	392
Number of RF cavities	8 per beam
Nominal energy, protons	6.5 TeV
Nominal energy, ions	2.56 TeV/u (energy per nucleon)
Nominal energy, protons collisions	13 TeV
No. of bunches per proton beam	2808
No. of protons per bunch (at start)	1.2×10^{11}
Number of turns per second	11245
Number of collisions per second	1 billion

Accelerator operation energies

Accelerator	Energy
Linac 2	50 MeV
PS Booster	1.4 GeV
Proton Scyncroton (PS)	25 GeV
SPS	450 GeV
LHC	6.5 TeV

Table. LHC characteristics for run 2.

CMS detector

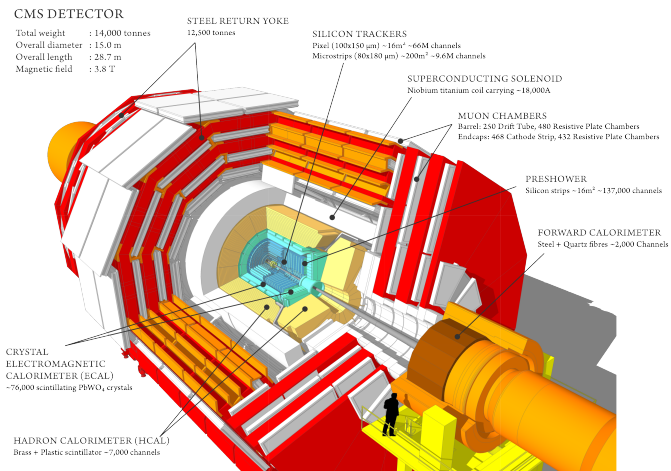
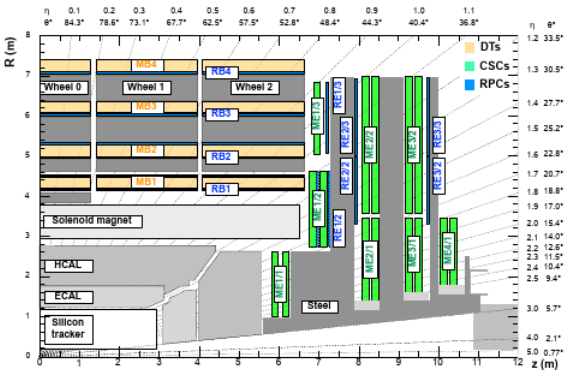


Figure: Compact muon solenoid

LHC



Slide view of the CMS in terms of pseudorapidity $\eta = -\ln [\tan(\frac{\theta}{2})]$

CMS integrated luminosity

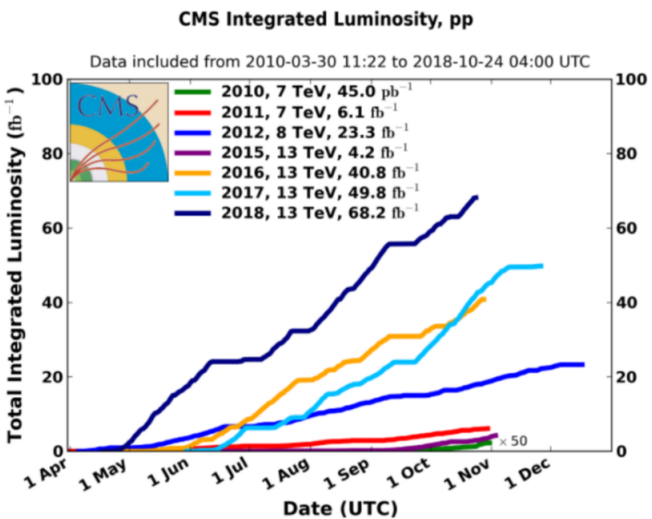
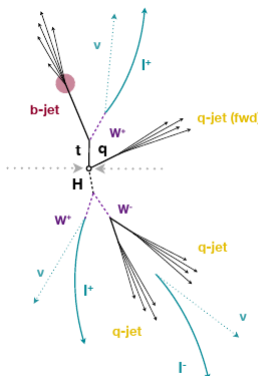


Figure: Integrated luminosity for CMS experiment

Topology of events tH

The characteristics of the signal tH :

- $t \rightarrow W^+ b \rightarrow l^+ \nu_\mu b$
 - $H \rightarrow W^+ W^-$
 - $W \rightarrow l^\pm \nu$, where l can be μ^\pm, e^\pm, τ^\pm
 - $W \rightarrow q\bar{q}$
 - W bosons decay leptonically resulting in a signature of two same-sign leptons
 - a light-flavor quark
 - A b-jet

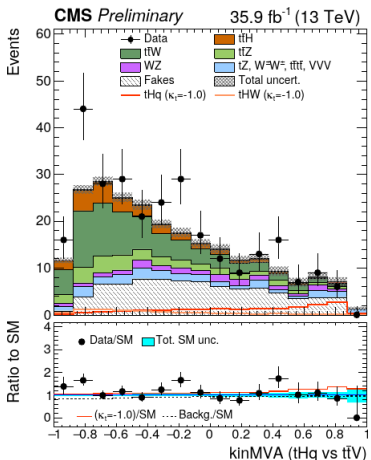


Event selection

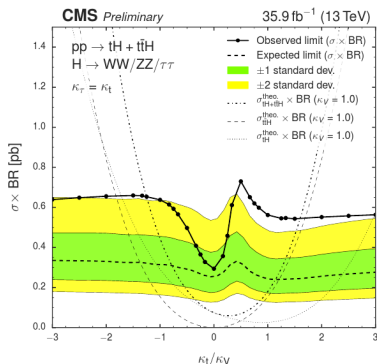
In order to detect signal events and reject background, the following selections are applied.

- The events must contain two muons with the same sign.
 - Transverse moment $p_t > 25$ GeV for the highest p_t muon and $p_t > 15$ GeV for the lowest p_t muon.
 - A forward jet with $p_t > 40$ GeV and $|\eta| > 2.4$
 - One or more b-tagged jets with $|\eta| < 2.4$

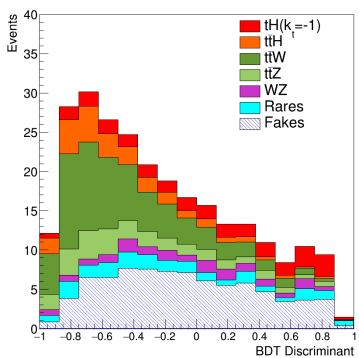
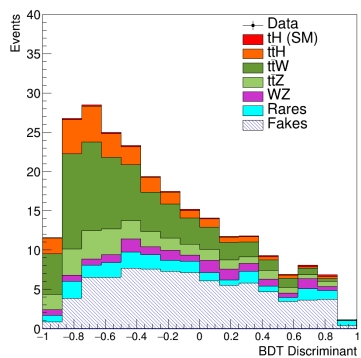
Previous results for $t\bar{t}H+tH$ production



Pre-fit classifier outputs for same sign dimuon, for training against $t\bar{t}V$



Observed and expected 95% C.L. upper limit on the $tH + t\bar{t}H$ cross section times $H \rightarrow WW + \tau\tau + ZZ$ branching fraction for different 20 values of the coupling ratio κ_t/κ_V . The expected limit is derived from a background-only MC dataset.



SM signal and backgrounds (Left) and $k_t = -1$ model (Right).

Main backgrounds

Table: Main backgrounds and their same sign $\mu\mu$ decay process

Background	Decay process
$t\bar{t}W$	$t\bar{t}W \rightarrow W^+ b W^- \bar{b} \mu^+ \nu_\mu \rightarrow \mu^+ \nu_\mu b \mu^- \bar{\nu}_\mu \bar{b} \mu^+ \nu_\mu$
$t\bar{t}Z$	$t\bar{t}Z \rightarrow W^+ b W^- \bar{b} \mu^+ \mu^- \rightarrow \mu^+ \nu_\mu b \mu^- \bar{\nu}_\mu \bar{b} \mu^+ \mu^-$
$W^+ Z$	$W^+ Z \rightarrow \mu^+ \nu_\mu \mu^+ \mu^-$
$W^\pm W^\pm$	$W^+ W^+ \rightarrow \mu^+ \nu_\mu \mu^+ \nu_\mu$
tZq	$tZq \rightarrow W^+ b \mu^+ \mu^- q \rightarrow \mu^+ \nu_\mu b \mu^+ \mu^- q$
$t\bar{t}t\bar{t}$	$t\bar{t}t\bar{t} \rightarrow W^+ b W^- \bar{b} W^+ b W^- \bar{b} \rightarrow \mu^+ \nu_\mu b \mu^- \bar{\nu}_\mu \bar{b} \mu^+ \nu_\mu b \mu^- \bar{\nu}_\mu \bar{b}$
$W^+ W^- Z$	$W^+ W^- Z \rightarrow \mu^+ \nu_\mu \mu^- \bar{\nu}_\mu \mu^+ \mu^-$
ZZZ	$ZZZ \rightarrow \mu^+ \mu^- \mu^+ \mu^- l^+ l^-$
$W^+ ZZ$	$W^+ ZZ \rightarrow \mu^+ \nu_\mu \mu^+ \mu^- l^+ l^-$
tZW^+	$tZW^+ \rightarrow W^+ b \mu^+ \mu^- \mu^+ \nu_\mu \rightarrow \mu^+ \nu_\mu b \mu^+ \mu^- \mu^+ \nu_\mu$
ZZ	$ZZ \rightarrow \mu^+ \mu^- \mu^+ \mu^-$
$t\bar{t}H$	$t\bar{t}H \rightarrow W^+ b W^- \bar{b} W^+ W^- \rightarrow \mu^+ \nu_\mu b \mu^- \bar{\nu}_\mu \bar{b} \mu^+ \nu_\mu \mu^- \bar{\nu}_\mu$

Signal and Backgrounds

Event yields for signal and backgrounds after the event selection for a integrated luminosity of 35.9 fb^{-1} . The uncertainties of yields include statistical and systematic [2]

Process	Number of events
$t\bar{t}W$	68 ± 10
$t\bar{t}Z$	25.9 ± 3.9
WZ	15.1 ± 7.7
Rares	20.9 ± 4.9
Fakes	80.9 ± 9.4
$t\bar{t}H$	24.2 ± 2.1
tH (SM)	2.14 ± 0.13
tH ($k_t = -1$)	26.2 ± 2.2

Systematic uncertainties

- The uncertainties on $t\bar{t}W$ and $t\bar{t}Z$ event yields are mainly due to the uncertainties of their production cross sections.
 - The uncertainty on WZ background is estimated using real data events in a three lepton control region.
 - In the Rare backgrounds, which are not measured, a 50% of uncertainty is assigned.
 - The uncertainty on the Fakes background is estimated using real data in a control region, defined by the muon identification criteria.
 - For the Higgs processes tH and ttH , the uncertainty are due to the theoretical parameters used in that simulation.

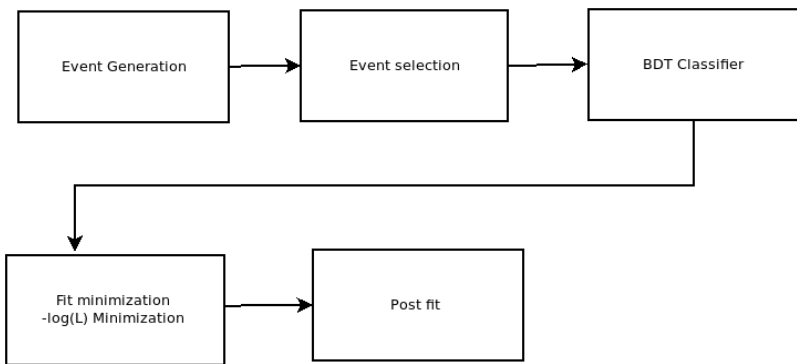
Boosted decision tree (BDT)

- A decision tree takes a set of input features and splits input data recursively based on those features. Boosting is a method of combining many weak learners (trees) into a strong classifier. The features can be a mix of categorical and continuous data.
 - The BDT training is performed using several event variables for signal and background.

BDT Variables

- Trailing lepton p_t
 - Total charge of tight leptons
 - $\min \Delta R$ (lepton pairs)
 - $\Delta\phi$ between highest p_t lepton pair
 - Number of jets with $|\eta| < 2.4$
 - Number of non b-tagged jets with $|\eta| > 1.0$
 - Maximum $|\eta|$ for jets
 - $\Delta\eta$ (most forward light jet, closest lepton)
 - $\Delta\eta$ (most forward light jet, hardest loosely b-tagged jet)
 - $\Delta\eta$ (most forward light jet, 2nd hardest loosely b-tagged jet)

Fitting



Likelihood model

The likelihood function is the product of Poisson probabilities for all bins

$$L(\mu, \alpha) = \prod_{j=1}^N \frac{(\mu s_j + b_j)^{n_j}}{n_j!} e^{-(\mu s_j + b_j)} \prod_{k=1}^M e^{\frac{-\alpha_k^2}{2}} \quad (6)$$

where N is the total number of bins, n_j is the number of events in a bin j , s_j is the number of signal events, μ is a parameter that modifies the signal strength and b_j is the number of background events. b_j is the sum of different background processes k

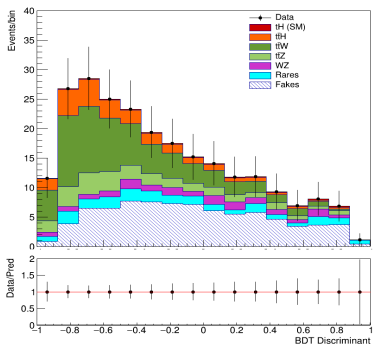
$$b_j = \sum_k^M b_j^k (1 + \alpha_k \sigma_k) \quad (7)$$

α_k is the parameter that modifies the expected background prediction and σ_k is the systematic uncertainty of the associated background. σ_k for the backgrounds are shown in the Table of yields.

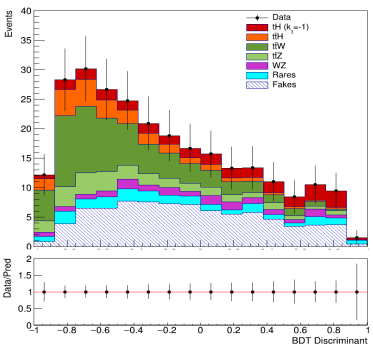
Results

The fit is applied by minimizing the $-\log L$ (NLL) with respect to the parameter μ and α_k . The minimization is performed by using the package ROOFIT. In the next slides, it shows the results of the model fitting using the Asimov data for the SM and the $k_t = -1$.

Results



Post-fit signal and background yields for tH process in the SM. In the box below each distribution, the ratio of the observed and event yields is shown



Post-fit signal and background yields for tH process in the $k_t = -1$. In the box below each distribution, the ratio of the observed and event yields is shown

Results

Table: Prefit and postfit table for each yield.

Process	Number of events prefit	Number of events Postfit
tH	2.13	5.33 ± 27.39
t <bar>t>H</bar>	24.18 ± 2.26	24.81 ± 2.24
t <bar>t>W</bar>	68.03 ± 9.54	76.99 ± 8.76
t <bar>t>Z</bar>	25.89 ± 3.20	26.74 ± 3.18
Rares SM	18.33 ± 9.23	20.31 ± 9.26
WZ	15.07 ± 7.59	15.94 ± 7.46
fakes	80.94 ± 40.86	100.16 ± 29.32

Prefit uncertainty is statistical only. Postfit uncertainty is statistical + systematic.

Results

Table: Prefit and postfit table for each yield. $k_t = -1$.

Process	Number of events prefit	Number of events Postfit
tH	26.2	1.83 ± 26.63
t <bar>t>H</bar>	24.18 ± 2.26	24.82 ± 2.27
t <bar>t>W</bar>	68.03 ± 9.54	77.07 ± 8.99
t <bar>t>Z</bar>	25.89 ± 3.20	26.76 ± 3.18
Rares SM	17.17 ± 8.64	18.90 ± 8.37
WZ	16.23 ± 8.17	17.54 ± 8.15
fakes	80.94 ± 40.86	102.97 ± 29.51

Prefit uncertainty is statistical only. Postfit uncertainty is statistical + systematic.

Results

Likelihood scan

Due to the large background, the signal strength for the Asimov data with 35.9 fb^{-1} is consistent with zero. Therefore, we estimate an upper limit on the signal strength at 95% confidence level.

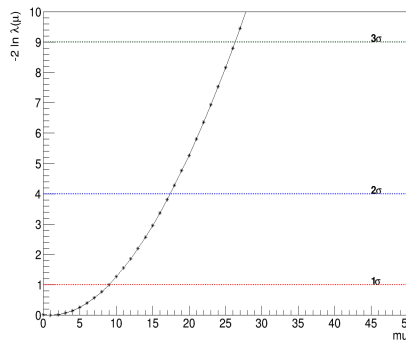
We can define the likelihood ratio

$$\lambda(\mu, \alpha) = \frac{L(\mu, \alpha)}{L(\hat{\mu}, \hat{\alpha})} \quad (8)$$

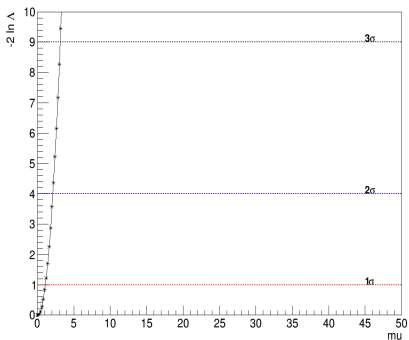
Where $\hat{\alpha}$ and $\hat{\mu}$ are the parameters obtained in the previous section which correspond to the minimal of the NLL.

Results

Likelihood scan

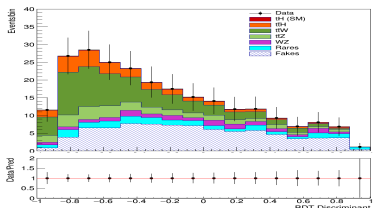


Likelihood scan for $k_t=1$ (SM)

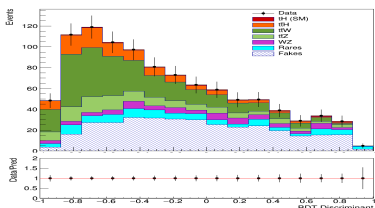


Likelihood scan for $k_t = -1$

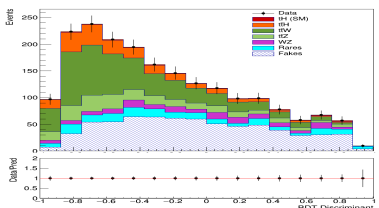
Extrapolation of luminosity for SM



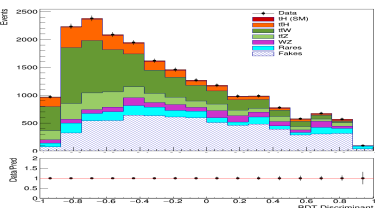
35.9 fb⁻¹



150 fb⁻¹

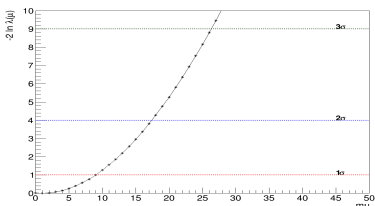


300 fb⁻¹

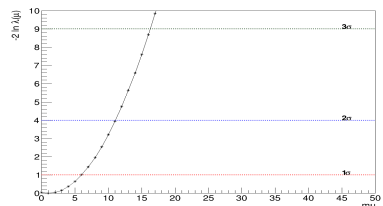


3000 fb^{-1}

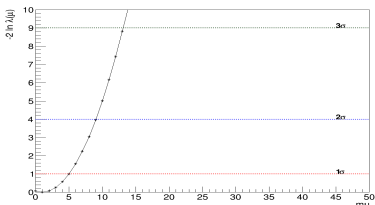
Likelihood scan for SM



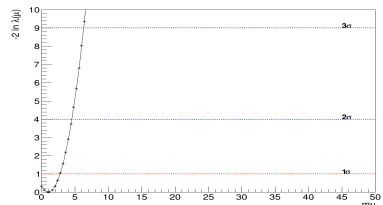
35.9 fb⁻¹



150 fb⁻¹

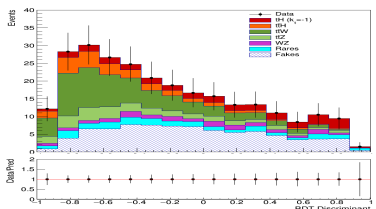


300 fb⁻¹

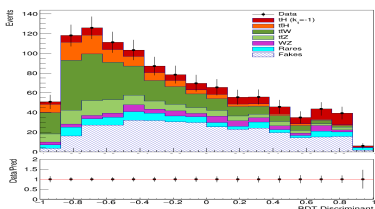


$\sim 3000 \text{ fb}^{-1}$

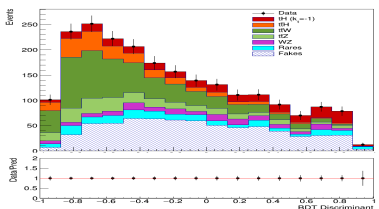
Extrapolation of luminosity for $k_t = -1$



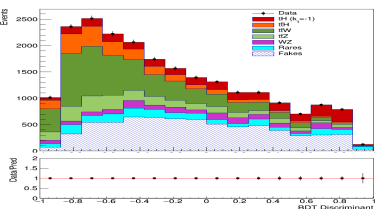
35.9 fb⁻¹



150 fb⁻¹

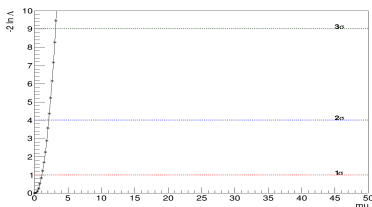


300 fb⁻¹

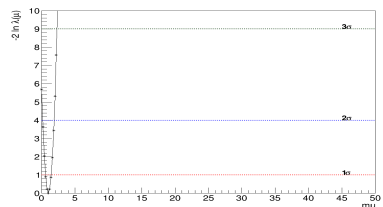


3000 fb^{-1}

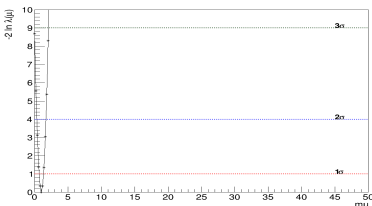
Likelihood scan for $k_t = -1$



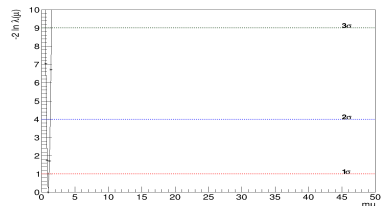
35.9 fb⁻¹



150 fb⁻¹



300 fb⁻¹



$\sim 3000 \text{ fb}^{-1}$

Results

Upper limit

To determine an upper limit on the strength parameter μ , we use the following statistical test

$$q(\mu, \alpha) = -2 \ln \lambda \quad (9)$$

High values of q represent greater incompatibility between the data and the fit model. q is a random variable with a χ^2 distribution.

Results

Results of μ and upper limits for Asimov extrapolations for SM and $k_t = -1$ models.

Luminosity (fb $^{-1}$)	μ (SM)	μ (SM) upper limit	μ ($k_t = -1$)	μ ($k_t = -1$) upper limit
35.9	1.0 ± 7.7	17	1.0 ± 0.5	2.3
150	1.0 ± 6.7	11	1.0 ± 0.4	1.8
300	1.0 ± 4.3	8.7	1.0 ± 0.3	1.5
3000	1.0 ± 1.7	4.3	1.0 ± 0.1	1.1

Conclusions

- We analyzed the tH process produced from PP collisions for the production of $\mu\mu$ final states
 - We discussed about events selections for the 2016 Run 2 from CMS.
 - The creation of an Asimov model with systematic uncertainties to make a minimization (fit) and obtain a fit which is compatible with Standard Model.
 - Generation of likelihood scan for the exclusion of data and obtain the probability of detection of a Higgs boson.
 - Generating simulations for predict results with higher luminosities, according to the future experiments.

Conclusions

- The results of the analysis for the SM case indicates that it is impossible to detect a Higgs boson using same sign dimuon channel in the tH process due to the low number of events and a huge uncertainty.
 - For the SM scenario the expected uncertainty even at the largest luminosities is not enough to observe the signal and only an upper limit can be placed.
 - For the $k_t = -1$, the uncertainty is low due to higher number of events for tH process and it is possible to detect a Higgs boson, but this model is purely theoretical and not related with the SM.
 - It requires a new analysis that includes more channels such as three leptons in the final state for improve the sensibility of the signal.

References

- Gross F. *Relativistic quantum mechanics and field theory*, 1994, WILEY-VCH Verlag GmbH & Co. KGaA
 - Griffiths, D. *Introduction to Elementary Particles*, 2nd edition, 2008, WILEY-VCH Verlag GmbH & Co. KGaA
 - The CMS collaboration, *Search for production of a Higgs boson and a single top quark in multilepton final states in proton collisions at 13 TeV*, CMS-HIG-18-009, Phys. Rev. D 99, 092005
 - Verkerke W *Dealing with systematic uncertainties* 2014. From https://indico.cern.ch/event/287744/contributions/1641261/attachments/535763/738679/Verkerke_Statistics_3.pdf

-  ATLAS and CMS Collaborations, *Combined measurement of the Higgs boson mass in pp collisions at $\sqrt{s} = 7$ and 8 TeV with the ATLAS and CMS experiments*, Phys. Rev. Lett. 114 (2015)
doi:10.1103/PhysRevLett.114.191803, arXiv:1503.07589
-  Cowan G. , Cranmer K., Gross E. , Vitells O. *Asymptotic formulae for likelihood-based tests of new physics* 2013 , arXiv:1007.1727
-  CMS collaboration *Search for tHq production in multilepton final states at 13 TeV* ,2017,CMS AN-16-378
-  CMS collaboration *High-Luminosity Large Hadron Collider (HL-LHC)*, 2017,CERN-2017-007-M

Back up

Sources of uncertainty on event yields

- Luminosity measurement: 2.6%.
 - Data/MC scale factors for lepton selection (ID, iso) and trigger efficiencies 5% per lepton.
 - Choice of PDF set:
 - 3.7% for tHq
 - 4% for tHW, t \bar{t} W, t \bar{t} Z, t \bar{t} H
 - Scale uncertainties: 12%, 4 for t \bar{t} W, 10% for t \bar{t} Z, +5.8/-9.2% for t \bar{t} H.
 - Background: WZ, ZZ sample modelling and statistics: 50%.
 - Rare SM (tZ, tri-bosons, WWqq, tt $\tau\tau$) : 50%
 - Fake rate estimation: The predicted event yield has a normalization uncertainty of 30-50% [7]

Sources of systematic uncertainty

Detector-simulation related uncertainty

- Calibrations (electron, jet energy scale)
 - Efficiencies (particle ID, reconstruction)
 - Resolutions (jet energy, muon momentum)

Theoretical uncertainties

- Factorization/Normalization scale of MC generators
 - Choice of MC generator (ME and/or PS, e.g. Herwig vs Pythia)

Monte Carlo Statistical uncertainties

- Statistical uncertainty of simulated samples[2]

Results

Likelihood scan

- Likelihood function (often simply the likelihood) is a function of the parameters of a statistical model, given specific observed data.
- Likelihood functions play a key role in frequentist inference, especially methods of estimating a parameter from a set of statistics.
- In informal contexts, "likelihood" is often used as a synonym for probability.

NLL